

# The $\gamma$ -band of $^{16}\text{O}_2$ , $^{16}\text{O}^{17}\text{O}$ , $^{17}\text{O}_2$ and $^{18}\text{O}_2$

H. Naus, K. Navaian, W. Ubachs \*

*Laser Centre, Department of Physics and Astronomy, Vrije Universiteit, De Boelelaan 1081, 1081 HV Amsterdam, Netherlands*

Received 14 July 1998; received in revised form 19 August 1998; accepted 2 October 1998

---

## Abstract

The  $b^1\Sigma_g^+ - X^3\Sigma_g^-$  (2,0) band of the  $^{16}\text{O}_2$ ,  $^{16}\text{O}^{17}\text{O}$ ,  $^{17}\text{O}_2$  and  $^{18}\text{O}_2$  oxygen isotopomers was investigated by means of cavity-ring-down laser spectroscopy. Line positions of the four branches in each band were determined with an accuracy of  $0.01\text{ cm}^{-1}$ . Improved or new molecular constants are derived for the  $b^1\Sigma_g^+$ ,  $v = 2$  excited state of the four isotopomers. © 1999 Elsevier Science B.V. All rights reserved.

**Keywords:**  $\gamma$ -Band; Cavity-ring-down laser spectroscopy; Isotopomers

---

## 1. Introduction

The oxygen ' $\gamma$ -band' is a very weak absorption feature, corresponding to the (2,0) band of the  $b^1\Sigma_g^+ - X^3\Sigma_g^-$  electronic system of the  $\text{O}_2$  molecule. This  $\gamma$ -band is a highly forbidden transition, since it is a gerade–gerade,  $\Sigma^+ - \Sigma^-$  and a singlet–triplet transition, while also the Franck–Condon factor for the (2,0) band is very small (0.00264) [1]. This magnetic-dipole-allowed transition has an oscillator strength of only  $0.63 \times 10^{-12}$ , but is despite its weakness (375 times weaker than the oxygen 'A-band'), a pronounced absorption feature readily observed in the Earth's atmosphere. In fact the first spectroscopic study of this  $\gamma$ -band was performed through absorption in a large air mass in the Earth's atmosphere at sunset [2].

From spectroscopic measurements on atmospheric ozone isotopic ratios in  $\text{O}_3$  were found to deviate from the terrestrial abundance of oxygen isotopes [3,4]. This phenomenon was ascribed to dynamical processes occurring in the atmosphere. To gain deeper understanding of these processes it is of importance to identify transitions by which the isotopic constitution of oxygen bearing molecules can be determined. The  $b^1\Sigma_g^+ - X^3\Sigma_g^-$  electronic system is such a tool to probe  $\text{O}_2$ -isotopomers in the Earth's atmosphere, as was demonstrated by Osterbrock et al. [5] and by Slinger et al. [6].

In the present work we report on a high resolution spectroscopic study of the oxygen  $\gamma$ -band, using the experimental technique of cavity-ring-down spectroscopy (CDRS) [7]. This technique was previously used in an investigation of the oxygen Herzberg bands in the ultraviolet [8] and, in our laboratory, for an investigation of the A-band for all isotopomers of  $\text{O}_2$  [9] as well as for

---

\* Corresponding author. Tel.: +31-20-4447948; fax: +31-20-4447999.

E-mail address: wimu@nat.vu.nl (W. Ubachs)

the B-band [10]. We present results for  $^{16}\text{O}_2$ ,  $^{16}\text{O}^{17}\text{O}$ ,  $^{18}\text{O}_2$  and  $^{17}\text{O}_2$ . For  $^{16}\text{O}_2$  the presently obtained accuracy is similar to that of the old work of Babcock and Herzberg [2], although the conditions in our laboratory experiment are better controlled, allowing for an improved assessment of pressure shifts. The  $\gamma$ -band of  $^{16}\text{O}_2$  was investigated by Wheeler et al. [11], also using CDRS, however without focusing on accurate calibration of the oxygen resonance lines. For  $^{18}\text{O}_2$  the  $\gamma$ -band was previously studied by Hill and Schawlow [12] and by Engeln et al. [13] with a slightly lower accuracy. For  $^{16}\text{O}^{17}\text{O}$  and  $^{17}\text{O}_2$  no results exist in the literature. New spectroscopic constants for the  $\text{b}^1\Sigma_g^+$ ,  $v=2$  state of the various  $\text{O}_2$ -isotopomers are derived, while in case of  $^{17}\text{O}_2$  also improved rotational constants for the  $\text{X}^3\Sigma_g^-$ ,  $v=0$  ground state are derived. These data allow for improved predictions of the positions of various bands, such as  $\text{b}^1\Sigma_g^+ - \text{X}^3\Sigma_g^-$  ( $2, v''$ ), which may be useful for future analysis of atmospheric emission phenomena.

## 2. Spectroscopic results on $^{16}\text{O}_2$ , $^{16}\text{O}^{17}\text{O}$ , $^{18}\text{O}_2$ and $^{17}\text{O}_2$

The experimental method used in the present study is similar to the one applied previously for the investigation of the oxygen A and B-bands [9,10]. Pulsed laser radiation of 5 ns duration is obtained from a Nd-YAG pumped dye laser system (Quanta-Ray PDL-3) running on DCM dye, allowing for tunability in the relevant wavelength range 625–640 nm. For the general principles of CDRS we refer to Refs. [7,11]. Specifics for the present investigation are mirrors with reflectivities of 99.98% and radii of curvature of 1 m forming a stable cavity at a mirror separation of 45 cm. Spectral recordings of the  $\text{O}_2$ -isotopomers were obtained by averaging five decay transients and on-line evaluation of the cavity decay time as a function of wavelength.

The spectrum of  $^{16}\text{O}_2$  was obtained from a natural gas sample, while spectral recordings of  $^{16}\text{O}^{17}\text{O}$  and  $^{17}\text{O}_2$  were obtained from a 50%  $^{17}\text{O}$ -

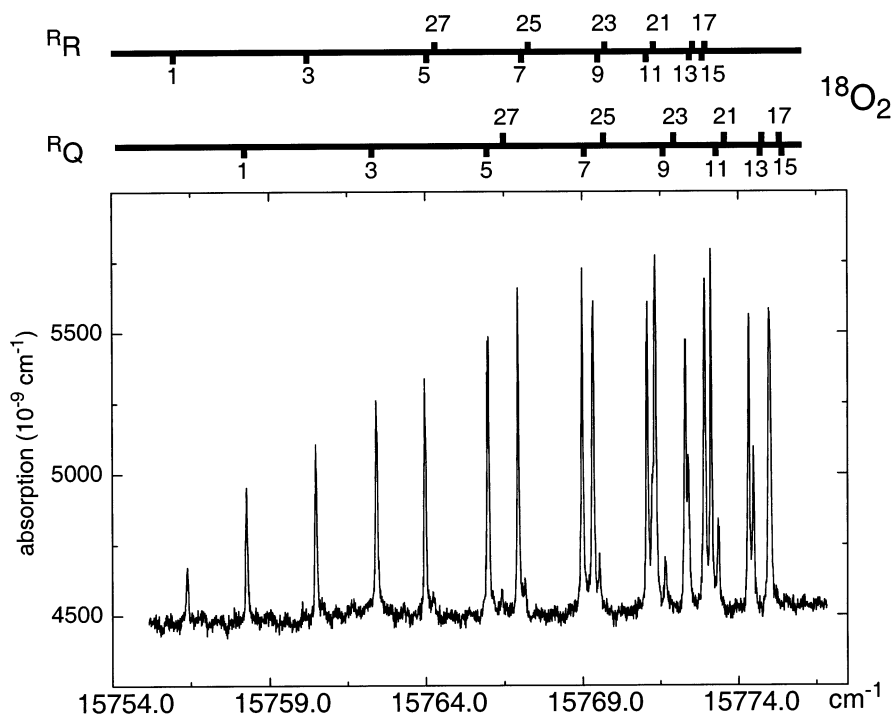


Fig. 1. Cavity-ring-down spectral recording of the R-bandhead of  $^{18}\text{O}_2$  obtained from an enriched sample.

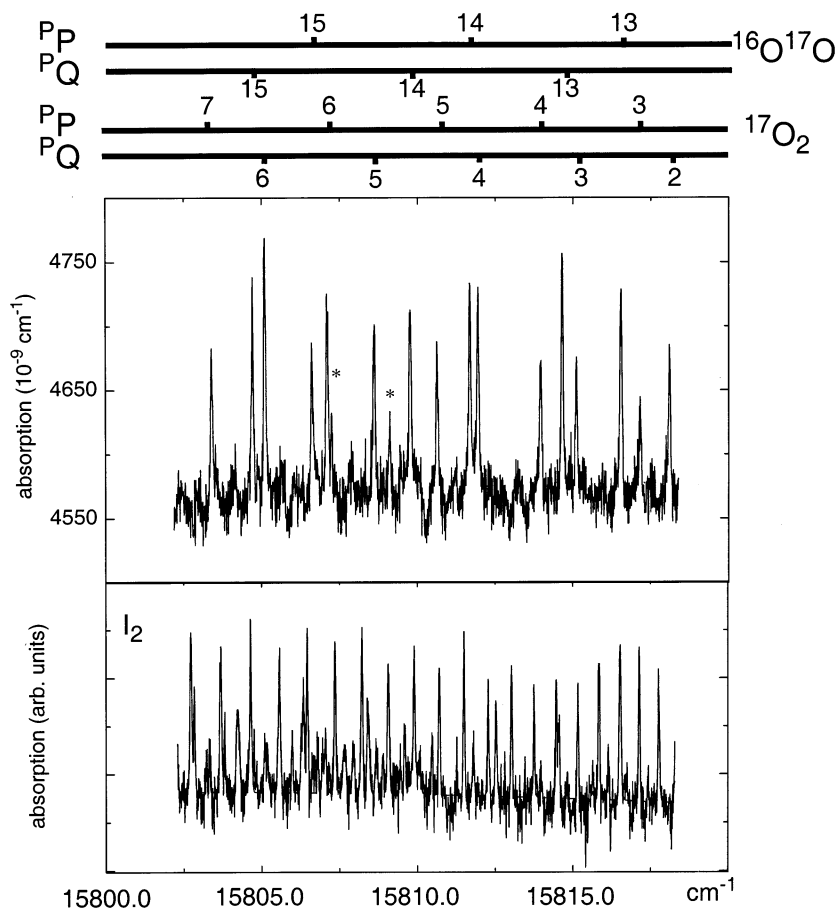


Fig. 2. Observed spectrum from a  $^{17}\text{O}$  (50% atom) enriched sample showing resonances pertaining to  $^{16}\text{O}^{17}\text{O}$  and  $^{17}\text{O}_2$ . Resonances indicated with (\*) belong to  $^{16}\text{O}_2$ . The spectrum in the lower panel is the simultaneously recorded  $\text{I}_2$ -absorption spectrum.

enriched oxygen sample (Campro Scientific) and  $^{18}\text{O}_2$  from a 95% enriched sample (Eurisotop). The spectra of  $^{16}\text{O}_2$  were recorded using typical pressures of 60 Torr in the cell, while in case of the enriched samples pressures of 200 Torr were applied. Signals of  $^{16}\text{O}^{18}\text{O}$  and  $^{17}\text{O}^{18}\text{O}$ , observed for the A and B-bands [9,10], were in case of the  $\gamma$ -band too weak to be reliably detected. Since the available mirrors at 630 nm have a lower reflectivity than the set available at 760 nm, the noise-equivalent detection limit at 630 nm is a factor of 10 higher at  $1 \times 10^{-8} \text{ cm}^{-1}$ , thus prohibiting observation of weaker features. We note that the  $\gamma$ -band is a factor of 375 weaker than the A-band [1]. Fig. 1 shows a spectrum of part of the R-band-head of  $^{18}\text{O}_2$ . In Fig. 2 a spectrum measured from

the  $^{17}\text{O}$  enriched sample is presented, showing  $^{16}\text{O}^{17}\text{O}$  and  $^{17}\text{O}_2$  resonances. Here also an on-line measured  $\text{I}_2$ -calibration spectrum is displayed.

Wavelength calibration of the oxygen lines is the central issue of this paper. For this purpose  $\text{I}_2$ -absorption spectra were recorded simultaneously with the oxygen spectra. To obtain a good signal-to-noise ratio on the  $\text{I}_2$ -spectra, the  $\text{I}_2$ -sample in a glass cell was heated to  $30^\circ\text{C}$ , thus reaching a vapour pressure of 1 Torr. Three passes through the 40 cm long cell, with normalization to a power spectrum of the laser output and averaging over five laser pulses, was sufficient to record typical  $\text{I}_2$ -absorption spectra at 630 nm, as displayed in the lower panel of Fig. 2. Gaussian curves were fitted to the  $\text{I}_2$ -resonances and after

assignment with the I<sub>2</sub>-reference atlas [14] a spline interpolation between the fitted I<sub>2</sub>-lines provides an accurate frequency scale for the simultaneously recorded oxygen spectrum. The O<sub>2</sub> resonances were then fitted to Voigt profiles. With linewidths in the I<sub>2</sub> and O<sub>2</sub>-spectra of 0.06 cm<sup>−1</sup>, predominantly caused by the laser bandwidth, this results in an absolute accuracy for strong and non-overlapped

O<sub>2</sub>-lines of 0.01 cm<sup>−1</sup>. In the I<sub>2</sub>-atlas the energy range 15 789–15 806 cm<sup>−1</sup> is missing due to interference with the HeNe-laser line during the production of the atlas. Therefore an interpolation over that range had to be made during the present measurements without being able to correct for nonlinearities in the scan. This explains the offset of the <sup>P</sup>Q(23) and <sup>P</sup>P(23) lines of <sup>16</sup>O<sub>2</sub> by 0.06 cm<sup>−1</sup>.

Table 1

The  $\gamma$ -band of <sup>16</sup>O<sub>2</sub>

| N  | <sup>P</sup> Q         |                | <sup>P</sup> P         |                | <sup>R</sup> R         |                | <sup>R</sup> Q         |                |
|----|------------------------|----------------|------------------------|----------------|------------------------|----------------|------------------------|----------------|
|    | Observed               | $\Delta_{o-c}$ | Observed               | $\Delta_{o-c}$ | Observed               | $\Delta_{o-c}$ | Observed               | $\Delta_{o-c}$ |
| 1  | *                      | *              | 15899.534              | −0.007         | 15907.660              | −0.009         | 15909.549              | 0.004          |
| 3  | 15895.372              | −0.005         | 15893.311              | 0.019          | 15912.259              | 0.004          | 15914.206              | 0.001          |
| 5  | 15888.392              | 0.000          | 15886.376              | −0.005         | 15916.179              | 0.004          | 15918.167              | 0.004          |
| 7  | 15880.784              | 0.004          | 15878.814              | 0.008          | 15919.432              | 0.005          | 15921.446              | 0.004          |
| 9  | 15872.514              | −0.001         | 15870.570              | 0.000          | 15922.005              | −0.003         | 15924.037              | −0.010         |
| 11 | 15863.601              | 0.009          | 15861.658              | −0.012         | 15923.911              | −0.005         | 15925.975              | −0.003         |
| 13 | 15853.985              | −0.023         | 15852.102              | −0.006         | 15925.144              | −0.006         | 15927.234              | 0.002          |
| 15 | 15843.768              | 0.005          | 15841.871              | −0.012         | 15925.705              | −0.001         | 15927.828              | 0.020          |
| 17 | 15832.853              | −0.002         | 15831.011              | 0.017          | 15925.579              | −0.003         | 15927.719              | 0.016          |
| 19 | 15821.282              | 0.000          | 15819.438              | −0.002         | 15924.761              | −0.014         | 15926.916              | 0.002          |
| 21 | 15809.036              | −0.007         | 15807.218              | −0.001         | 15923.282 <sup>b</sup> | 0.001          | 15925.442              | 0.004          |
| 23 | 15796.060 <sup>a</sup> | −0.077         | 15794.279 <sup>a</sup> | −0.052         | 15921.101              | 0.005          | 15923.282 <sup>b</sup> | 0.010          |
| 25 | 15782.560              | −0.002         | 15780.785              | 0.011          |                        |                |                        |                |
| 27 | 15768.324              | 0.009          | 15766.526              | −0.019         |                        |                |                        |                |

<sup>a</sup> Due to missing part in I<sub>2</sub>-atlas, calibration inaccurate.

<sup>b</sup> Blended line.

Table 2

The  $\gamma$ -band of <sup>18</sup>O<sub>2</sub>

| N  | <sup>P</sup> Q |                | <sup>P</sup> P |                | <sup>R</sup> R |                | <sup>R</sup> Q |                |
|----|----------------|----------------|----------------|----------------|----------------|----------------|----------------|----------------|
|    | Observed       | $\Delta_{o-c}$ | Observed       | $\Delta_{o-c}$ | Observed       | $\Delta_{o-c}$ | Observed       | $\Delta_{o-c}$ |
| 1  | *              | *              | 15749.142      | −0.004         | 15756.377      | −0.006         | 15758.292      | 0.000          |
| 3  | 15745.650      | −0.006         | 15743.610      | 0.006          | 15760.490      | 0.002          | 15762.442      | −0.011         |
| 5  | 15739.489      | 0.005          | 15737.477      | −0.010         | 15764.017      | 0.001          | 15766.006      | −0.005         |
| 7  | 15732.771      | 0.008          | 15730.797      | 0.001          | 15766.969      | 0.004          | 15768.986      | 0.002          |
| 9  | 15725.478      | 0.002          | 15723.536      | 0.004          | 15769.335      | 0.000          | 15771.377      | 0.003          |
| 11 | 15717.616      | −0.003         | 15715.708      | 0.013          | 15771.133      | 0.009          | 15773.190      | 0.009          |
| 13 | 15709.190      | 0.001          | 15707.279      | −0.005         | 15772.335      | 0.005          | 15774.408      | 0.004          |
| 15 | 15700.183      | −0.004         | 15698.298      | −0.001         | 15772.957      | 0.006          | 15775.035      | −0.007         |
| 17 | 15690.604      | −0.008         | 15688.727      | −0.013         | 15772.990      | 0.006          | 15775.080      | −0.012         |
| 19 | 15680.457      | −0.004         | 15678.606      | −0.001         | 15772.436      | 0.007          | 15774.555      | 0.002          |
| 21 | 15669.734      | −0.001         | 15667.886      | −0.011         | 15771.283      | 0.003          | 15773.432      | 0.011          |
| 23 | 15658.424      | −0.009         | 15656.610      | 0.000          | 15769.551      | 0.014          | 15771.698      | 0.004          |
| 25 | 15646.569      | 0.017          | 15644.737      | −0.008         | 15767.184      | −0.013         |                |                |
| 27 | 15634.086      | −0.005         | 15632.290      | −0.009         | 15764.265      | 0.010          | 15766.441      | −0.002         |

Table 3  
The  $\gamma$ -band of  $^{17}\text{O}_2$

| <i>N</i> | <sup>P</sup> Q         |                | <sup>P</sup> P         |                | <sup>R</sup> R         |                | <sup>R</sup> Q         |                |
|----------|------------------------|----------------|------------------------|----------------|------------------------|----------------|------------------------|----------------|
|          | Observed               | $\Delta_{o-c}$ | Observed               | $\Delta_{o-c}$ | Observed               | $\Delta_{o-c}$ | Observed               | $\Delta_{o-c}$ |
| 0        | *                      | *              | *                      | *              | *                      | *              | 15827.999              | −0.001         |
| 1        | *                      | *              | 15820.928              | −0.004         |                        |                | 15830.491              | 0.011          |
| 2        | 15820.230              | 0.008          | 15818.068              | −0.003         | 15830.848              | 0.018          | 15832.780              | 0.019          |
| 3        | 15817.132              | −0.003         | 15815.065              | 0.008          | 15832.911              | −0.007         | 15834.877 <sup>a</sup> | 0.002          |
| 4        | 15813.908              | −0.011         | 15811.884              | −0.005         | 15834.877 <sup>a</sup> | 0.026          | 15836.830              | 0.003          |
| 5        | 15810.575              | 0.003          | 15808.564              | −0.003         | 15836.633              | 0.003          | 15838.623              | 0.002          |
| 6        | 15807.077              | 0.000          | 15805.100              | 0.009          | 15838.239              | −0.014         | 15840.257              | −0.001         |
| 7        | 15803.424              | −0.008         | 15801.413 <sup>a</sup> | −0.048         | 15839.711              | −0.011         | 15841.726              | −0.012         |
| 8        | 15799.608              | −0.027         | 15797.665              | −0.013         | 15841.033              | −0.001         | 15843.083              | 0.021          |
| 9        | 15795.674              | −0.012         | 15793.736              | −0.005         | 15842.184              | −0.008         | 15844.231 <sup>a</sup> | 0.001          |
| 10       | 15791.578              | −0.006         | 15789.648              | −0.002         | 15843.216              | 0.023          | 15845.245 <sup>a</sup> | 0.003          |
| 11       | 15787.323              | −0.006         | 15785.410              | 0.004          | 15844.044              | 0.006          | 15846.093              | −0.004         |
| 12       | 15783.958 <sup>a</sup> | 0.037          | 15781.013              | 0.006          | 15844.729              | 0.001          | 15846.814              | 0.018          |
| 13       | 15778.366              | 0.007          | 15776.475              | 0.019          | 15845.245 <sup>a</sup> | −0.015         | 15847.342 <sup>a</sup> | 0.004          |
| 14       | 15773.659              | 0.015          | 15771.749              | −0.001         | 15845.621              | −0.015         | 15847.701 <sup>a</sup> | −0.022         |
| 15       | 15768.771              | −0.005         | 15766.886              | −0.005         | 15845.840 <sup>a</sup> | −0.015         | 15847.939 <sup>a</sup> | −0.012         |
| 16       | 15763.756              | 0.002          | 15761.887              | 0.009          | 15845.916              | −0.001         | 15848.012              | −0.009         |
| 17       | 15758.564              | −0.015         | 15756.706              | −0.006         | 15845.840 <sup>a</sup> | 0.019          | 15847.939 <sup>a</sup> | 0.005          |
| 18       | 15753.276              | 0.027          | 15751.394              | 0.003          | 15845.536 <sup>a</sup> | −0.032         | 15847.701 <sup>a</sup> | 0.011          |
| 19       | 15747.761              | −0.005         | 15745.919              | 0.002          | 15845.126 <sup>a</sup> | −0.030         | 15847.342 <sup>a</sup> | 0.055          |
| 20       | 15742.128              | −0.001         | 15740.271              | −0.018         | 15844.571              | −0.015         | 15846.730              | 0.005          |
| 21       | 15736.352              | 0.013          |                        |                | 15843.860              | 0.002          |                        |                |
| 22       |                        |                |                        |                |                        |                |                        |                |
| 23       |                        |                |                        |                | 15841.926              | 0.003          |                        |                |

<sup>a</sup> Blended line.

### 3. Data analysis

Line positions obtained from the computerized fitting and interpolation procedures are listed in Tables 1–4 for  $^{16}\text{O}_2$ ,  $^{16}\text{O}^{17}\text{O}$ ,  $^{18}\text{O}_2$  and  $^{17}\text{O}_2$ , respectively. The data were, for each isotopomer separately, included in a least-squares fit, to deduce molecular constants. Here the values were weighted with the estimated errors. For blended lines the uncertainties were taken higher than the nominal uncertainty of  $0.01\text{ cm}^{-1}$ . The effective Hamiltonian of Rouillé et al. [15] was used to describe the  $X^3\Sigma_g^-, v=0$  ground state. As in our previous studies the ground state constants were kept fixed at the accurate values derived from microwave and far-infrared spectroscopy [9]. For the  $b^1\Sigma_g^+, v=2$  excited state we use the representation:

$$E(N) = v_{20} + B'N(N+1) - D'N^2(N+1)^2 \quad (1)$$

The fitting routines then yield values and uncertainties ( $1\sigma$ ) for the  $v_{20}$ ,  $B'$  and  $D'$  molecular constants, which are listed in Table 5. The least-squares fits converge with standard deviations ranging from  $0.007$  to  $0.010\text{ cm}^{-1}$  (listed in Table 5). We note that the value of  $v_{20}$  is taken with respect to the zero energy as represented by the equations of Rouillé et al. This zero-level does not coincide with a particular quantum state, hence the band origins deviate by a certain amount from other studies. For  $^{17}\text{O}_2$  no accurate ground state constants are available from microwave or far-infrared spectroscopy. Therefore the present data on the  $\gamma$ -band are included in a combined fit with data pertaining to the A and B-bands [9,10] of our previous studies. In the fit to 266 points the

rotational constants of the ground state as well as three constants for each vibrational level in  $b^1\Sigma_g^+$  were varied resulting in updated values for the electronic ground state of  $^{17}\text{O}_2$ :  $B_0 = 1.35300$  (2)  $\text{cm}^{-1}$  and  $D_0 = 4.272$  (16)  $\times 10^{-6}$   $\text{cm}^{-1}$ . This procedure results in the constants for the excited state as listed in Table 5.

In principle the method of CDRS is suitable for determining absolute values of absorption strengths. The intensity-scales of Figs. 1 and 2 indeed represent absorption strengths in  $\text{cm}^{-1}$ , while the background level represents the (slightly wavelength-dependent) reflectivity of the mirrors. However the data have to be cautiously treated before an interpretation in terms of an absolute cross-section is valid. In cases where the bandwidth of the laser exceeds the Doppler or collision broadened linewidth the absolute in-

tensities in CDRS are systematically underestimated, as was discussed by Jongma et al. [16] and by Hodges et al. [17].

#### 4. Discussion and conclusion

From this CRDS-study, accurate line positions for the  $\gamma$ -band of four molecular oxygen isotopomers ( $^{16}\text{O}_2$ ,  $^{16}\text{O}^{17}\text{O}$ ,  $^{18}\text{O}_2$  and  $^{17}\text{O}_2$ ) and molecular constants for the  $b^1\Sigma_g^+$ ,  $v=2$  excited state result.

These recordings were taken in a laboratory environment at well-defined pressures, that were constant over the absorption path. Phillips and Hamilton [18] have determined pressure shifts, amounting to  $-0.011$   $\text{cm}^{-1}$   $\text{atm}^{-1}$  for the A-band and  $-0.014$   $\text{cm}^{-1}$   $\text{atm}^{-1}$  for the B-band.

Table 4  
The  $\gamma$ -band of  $^{16}\text{O}^{17}\text{O}$

| $N$ | $^{\text{P}}\text{Q}$<br>Observed | $\Delta_{o-c}$ | $^{\text{P}}\text{P}$<br>Observed | $\Delta_{o-c}$ | $^{\text{R}}\text{R}$<br>Observed | $\Delta_{o-c}$ | $^{\text{R}}\text{Q}$<br>Observed | $\Delta_{o-c}$ |
|-----|-----------------------------------|----------------|-----------------------------------|----------------|-----------------------------------|----------------|-----------------------------------|----------------|
| 1   | *                                 | *              | 15860.545                         | -0.015         | 15868.443                         | -0.008         | 15870.348                         | 0.013          |
| 2   | 15859.762                         | -0.012         | 15857.628                         | 0.019          | 15870.762 <sup>a</sup>            | 0.002          | 15872.693                         | 0.006          |
| 3   | 15856.602                         | 0.027          | 15854.480                         | -0.018         | 15872.942                         | 0.033          | 15874.870 <sup>a</sup>            | 0.007          |
| 4   | 15853.262                         | 0.000          | 15851.211                         | -0.017         | 15874.870 <sup>a</sup>            | -0.028         | 15876.871                         | 0.000          |
| 5   | 15849.798                         | -0.007         | 15847.798                         | 0.001          | 15876.726                         | 0.001          | 15878.720                         | 0.005          |
| 6   | 15846.187                         | -0.008         | 15844.214                         | 0.007          | 15878.393                         | 0.001          | 15880.401                         | 0.006          |
| 7   | 15842.425                         | -0.004         | 15840.454                         | -0.003         | 15879.903                         | 0.007          | 15881.908                         | -0.005         |
| 8   | 15838.496                         | -0.010         | 15836.542                         | -0.006         | 15881.241                         | 0.001          | 15883.254                         | -0.014         |
| 9   | 15834.427                         | 0.003          | 15832.481                         | 0.002          | 15882.425                         | 0.003          | 15884.466                         | 0.005          |
| 10  | 15830.185                         | 0.002          | 15828.247                         | -0.003         | 15883.423                         | -0.018         | 15885.508 <sup>a</sup>            | 0.017          |
| 11  | 15825.781                         | -0.003         | 15823.860                         | -0.001         | 15884.293                         | -0.006         | 15886.371 <sup>a</sup>            | 0.012          |
| 12  | 15821.232                         | 0.007          | 15819.309                         | -0.004         | 15884.999                         | 0.005          | 15887.067                         | 0.003          |
| 13  | 15816.504                         | -0.003         | 15814.611                         | 0.006          | 15885.508 <sup>a</sup>            | -0.018         | 15887.602                         | -0.003         |
| 14  | 15811.624                         | -0.006         | 15809.738                         | 0.000          | 15885.893                         | -0.002         | 15887.974                         | -0.010         |
| 15  | 15806.589                         | -0.004         | 15804.712                         | 0.002          | 15886.114 <sup>a</sup>            | 0.014          | 15888.230 <sup>a</sup>            | 0.031          |
| 16  | 15801.413                         | 0.017          | 15799.527                         | 0.004          | 15886.114 <sup>a</sup>            | -0.028         | 15888.230 <sup>a</sup>            | -0.020         |
| 17  | 15796.033 <sup>a</sup>            | -0.006         | 15794.168                         | -0.008         | 15886.022                         | 0.002          | 15888.143                         | 0.006          |
| 18  | 15790.521                         | -0.002         | 15788.651 <sup>a</sup>            | -0.017         | 15885.734                         | 0.001          | 15887.858                         | -0.001         |
| 19  | 15784.843                         | -0.003         | 15783.003                         | 0.002          | 15885.302                         | 0.020          | 15887.426                         | 0.009          |
| 20  | 15779.013                         | 0.003          | 15777.173                         | 0.000          | 15884.678                         | 0.013          | 15886.818                         | 0.009          |
| 21  | 15773.041 <sup>b</sup>            | 0.028          | 15771.211                         | 0.026          |                                   |                | 15886.022 <sup>a</sup>            | -0.014         |
| 22  | 15766.886 <sup>a</sup>            | 0.031          | 15765.021                         | -0.015         | 15882.939                         | 0.003          | 15885.084                         | -0.013         |
| 23  | 15760.527                         | -0.010         |                                   |                | 15881.812                         | -0.009         |                                   |                |
| 24  |                                   |                |                                   |                | 15880.540                         | 0.000          |                                   |                |

<sup>a</sup> Blended line.

<sup>b</sup> Calibration problem due to extrapolation.

Table 5  
Molecular constants for the  $b^1\Sigma_g^+$ ,  $v = 2$  excited state of molecular oxygen<sup>a</sup>

|            | <sup>16</sup> O <sub>2</sub> | <sup>16</sup> O <sup>17</sup> O | <sup>18</sup> O <sub>2</sub> | <sup>17</sup> O <sub>2</sub> |
|------------|------------------------------|---------------------------------|------------------------------|------------------------------|
| $\nu_{20}$ | 15903.748 (3)                | 15864.681 (2)                   | 15753.033 (2)                | 15824.969 (3)                |
| $B$        | 1.35463 (2)                  | 1.31523 (2)                     | 1.20614 (2)                  | 1.27587 (3)                  |
| $D$        | 5.49 (3) $10^{-6}$           | 5.16 (4) $10^{-6}$              | 4.32 (2) $10^{-6}$           | 4.69 (5) $10^{-6}$           |
| $\sigma$   | 0.009                        | 0.010                           | 0.007                        | 0.010                        |

<sup>a</sup> The values for  $\nu_{20}$  are not corrected for possible pressure shifts (see text).  $\sigma$  represents the standard deviation of the fit. All values in  $\text{cm}^{-1}$ .

In a simple extrapolation a pressure shift of  $-0.017 \text{ cm}^{-1} \text{ atm}^{-1}$  would follow for the  $\gamma$ -band. For the present measurements conducted at pressures of 60 Torr (for <sup>16</sup>O<sub>2</sub>) this implies a pressure shift of  $-0.0013 \text{ cm}^{-1}$ , while for the <sup>16</sup>O<sup>17</sup>O, and <sup>17</sup>O<sub>2</sub> and <sup>18</sup>O<sub>2</sub> spectra a pressure shift of  $-0.005 \text{ cm}^{-1}$  may be expected assuming that the pressure shift is isotope independent. The values for  $\nu_{20}$  in Table 5 are not corrected for these pressure shifts.

For <sup>16</sup>O<sup>17</sup>O and <sup>17</sup>O<sub>2</sub> the present data are the first reported for the  $\gamma$ -band. For <sup>18</sup>O<sub>2</sub> the  $\gamma$ -band was previously studied by Hill and Schawlow [12], however without an absolute calibration. Relative frequency measurements yielded rotational constants  $B = 1.2067 (5) \text{ cm}^{-1}$  and  $D = 4.7 (5) \times 10^{-6} \text{ cm}^{-1}$ , in agreement with the present findings. Engeln et al. [13] did not perform a rotational analysis on their data for the  $\gamma$ -band of <sup>18</sup>O<sub>2</sub>. The old data of Babcock and Herzberg [2] are still considered the most accurate for the  $\gamma$ -band of <sup>16</sup>O<sub>2</sub>. It should be noted that the value for  $\nu_{20}$  given in Ref. [2] relates to the lowest  $N = 1$ ,  $J = 0$  level which is offset by  $1.3316 \text{ cm}^{-1}$  from the zero-level contained in the Hamiltonian of Rouillé et al. [15]. When corrected for this offset a value of  $15903.747 \text{ cm}^{-1}$  results for the band origin in the work of Babcock and Herzberg exactly coinciding with the present value. Since the data of Ref. [2] were obtained from atmospheric observations where most absorption occurs in a high density region, a corrected value for the band origin would be slightly blue-shifted from the present value.

In a recent study of the  $b^1\Sigma_g^+ - X^3\Sigma_g^- (3,0)$  band of <sup>16</sup>O<sub>2</sub> [19] a discrepancy was found with

the data of Ref. [2]. The value for the band origin of Ref. [2] was found to be red-shifted with respect to the value of Ref. [19]. This was attributed to a systematic error in Ref. [2]. The present results do not support the conclusion of a red-shift in the old data of Ref. [2].

### Acknowledgements

The authors acknowledge financial support from the Space Research Organization Netherlands (SRON). KN was on leave from Uppsala University within the EC undergraduate student program SOCRATES.

### References

- [1] V.D. Galkin, Opt. Spectrosc. 47 (1979) 151.
- [2] H.B. Babcock, L. Herzberg, Astrophys. J. 108 (1948) 167.
- [3] D. Krankowsky, K. Mauersberger, Science 274 (1996) 1324.
- [4] G.I. Gellene, Science 274 (1996) 1344.
- [5] D.E. Osterbrock, J.P. Fulbright, A.R. Martel, M.J. Keane, S.C. Trager, G. Basri, Astron. Soc. Pac. 108 (1996) 277.
- [6] T.G. Slanger, D.L. Huestis, D.E. Osterbrock, J.P. Fulbright, Science 277 (1997) 1485.
- [7] A. O'Keefe, D.A.G. Deacon, Rev. Sci. Instrum. 59 (1988) 2544.
- [8] T.G. Slanger, D.L. Huestis, P.C. Cosby, H. Naus, G. Meijer, J. Chem. Phys. 105 (1996) 9393.
- [9] H. Naus, A. de Lange, W. Ubachs, Phys. Rev. A56 (1997) 4755.
- [10] H. Naus, S.J. van der Wiel, W. Ubachs, J. Mol. Spectrosc. 192 (1998) 162.
- [11] M.D. Wheeler, S.N. Newman, A.J. Orr-Ewing, M. Ashfold, J. Chem. Faraday Trans. 94 (1998) 337.

- [12] W.T. Hill III, A.L. Schawlow, J. Opt. Soc. Am. B5 (1988) 745.
- [13] R. Engeln, G. von Helden, G. Berden, G. Meijer, Chem. Phys. Lett. 262 (1996) 105.
- [14] S. Gerstenkorn, P. Luc, in: CNRS (Ed.), Atlas du Spectre D'absorption de la Molecule de L'iode Entre 14 800–20 000  $\text{cm}^{-1}$ , CNRS, Paris, 1978.
- [15] G. Rouillé, G. Millot, R. Saint-Loup, H. Berger, J. Mol. Spectrosc. 154 (1992) 327.
- [16] R.T. Jongma, M.G.H. Boogaarts, I. Holleman, G. Meijer, Rev. Sci. Instrum. 66 (1995) 2821.
- [17] J.T. Hodges, J.P. Looney, R.D. van Zee, Appl. Opt. 35 (1996) 4112.
- [18] A.J. Phillips, P.A. Hamilton, J. Mol. Spectrosc. 174 (1995) 587.
- [19] L. Biennier, A. Campargue, J. Mol. Spectrosc. 188 (1998) 248.